Trans-membrane signal transduction and biochemical Turing pattern formation

Mark M. Millonas[1] and Erik M. Rauch[2]

[1]Molecular Biophysics Group, 2001 Stern Hall, Department of Physics,

Tulane University, New Orleans, LA 70118

[2]Artificial Intelligence Laboratory, Massachusetts Institute of Technology,

545 Technology Square, Cambridge MA 02139

September 8, 1999

The Turing mechanism[1] for the production of a broken spatial symmetry in an initially homogeneous system of reacting and diffusing substances has attracted much interest as a potential model for certain aspects of morphogenesis[2–4] such as pre-patterning in the embryo, and has also served as a model for self-organization in more generic systems.[5] The two features necessary for the formation of Turing patterns are short-range autocatalysis and long-range inhibition[6,7] which usually only occur when the diffusion rate of the inhibitor is significantly greater than that of the activator. This observation has sometimes been used

to cast doubt on applicability of the Turing mechanism to cellular patterning since many messenger molecules that diffuse between cells do so at more-or-less similar rates. Here we show that stationary, symmetry-breaking Turing patterns can form in physiologically realistic systems even when the extracellular diffusion coefficients are equal; the kinetic properties of the "receiver" and "transmitter" proteins responsible for signal transduction will be primary factors governing this process.

The class of mechanisms we study is schematized in Fig. 1. Below we give a specific example for the purpose of illustrating the generic features of the whole class of such systems. The model is realistic in the sense that it makes use of reactions and reaction kinetics of a type which can be found in every living cell. In the model, signal transduction across the cell membrane connects the genetically controlled biochemical reactions in the cytosol to the production of messenger molecules in the extracellular matrix. These then diffuse at approximately equal rates, thereby coupling the reactions taking place inside cells at different points in space. We have found that this coupling can allow Turing patterns to spontaneously form in collections of cells even if the messenger diffusion rates (D) are identical (or very similar). We therefore believe the chemically realistic class of mechanisms we describe here could be of some relevance to understanding certain aspects of cellular morphogenesis.

The simplified set of reactions taking place in the cytosol involve an "activator" substance A and an "inhibitor" substance I that are synthesized by the cell at the rates c_A and c_I respectively, and in turn are broken down by the cell at the rates λ_A and λ_I as shown in Fig.

1, where

$$d[A]/dt = c_A - \lambda_A[A], \qquad d[I]/dt = c_I - \lambda_I[I]. \tag{1}$$

Activator is also produced by the autocatalytic process

$$A + E_1 \rightleftharpoons E_1A \;\; (K_1 = [E_1][A]/[E_1A]), \;\; \psi + E_1A \xrightarrow{k_1} E_1A + A, \tag{2}$$

$$d[A]/dt = V_1[A]/(K_1 + [A]), \quad V_1 = [E_1]_c k_1,$$

where we will use ψ as a shorthand for substances from the large and constant concentration of assorted biochemical building blocks present in the cell that are used to synthesize A and I. The activator also catalyzes the production of more inhibitor through the set of reactions

$$A + E_2 \rightleftharpoons E_2A \;\; (K_2 = [E_2][A]/[E_2A]), \;\; \psi + E_2A \xrightarrow{k_2} E_2A + I, \tag{3}$$

$$d[I]/dt \simeq V_2[A]/K_2, \quad V_2 = [E_2]_c k_2,$$

where for simplicity we have assumed that this reactions operates well below saturation, with $[A] \ll K_2$. Lastly, the inhibitor suppresses the activator through the set of reactions

$$A + E_3 \rightleftharpoons E_3A \qquad (K_3 = [E_3][A]/[E_3A]), \tag{4}$$

$$I + E_3A \xrightarrow{k_3} E_3AI \rightarrow E_3\psi I \rightarrow E_3 + \psi + I,$$

$$-d[A]/dt = V_3[A][I]/(K_3 + [A]), \quad V_3 = [E_3]_c k_3.$$

The rates of the catalytic process are given by the Michaelis-Menten[8] kinetics, where K_i are the Michaelis constants, k_i the catalytic rates and V_i the limiting rates for the catalytic processes. The E_i's are catalysts of the reactions where $[E_i]_0$ are the total concentrations of these catalysts produced by the genetic machinery of the cell. Because of the need for enzymes, we assume these reactions, including the breakdown of A and I, can only occur inside the cell.

In addition to being biologically reasonable, our model differs from the classical Turing model in two important respects. First, it takes into account the fact that genetically regulated biochemical processes will take place inside the cell, while cell-to-cell interaction must involve some form of trans-membrane signalling, since most biomolecules are highly insoluble in the lipid matrix of the cell membrane. Secondly, the diffusion of the two messenger molecules through the extracellular matrix take place at identical rates D.

Since pre-patterning is likely to involve switching on different sets of genes in different cells, some mechanism must exist for signalling between the genes. Our model makes use of signal transduction kinetics diagrammed in Fig. 1, where α_A and α_I are the rates of production of the messenger molecules M_A and M_I. This process is mediated by *transmitter* proteins T_A and T_I in the membrane. In the figure, signal transduction is viewed as the transformation of A and I into M_A and M_I respectively (though transformation into messenger molecules is not a requirement of the model). Conversely, the β_A and β_I are the rates of transformation of M_A and M_I into A and I, a process mediated by R_A and R_I, the

receiver proteins. This simplified picture can stand for more complex signal transduction mechanisms since the basic features responsible for the self-organization of the system are generic. For example, the signal transduction could involve the binding of A or I to specific receptor proteins on the intracellular side of the membrane, triggering the release of messenger molecules on the extracellular side of the membrane which then carry the signal to other cells.

The cell essentially has nearly complete freedom to control the signal transduction kinetics, whose associated rates could quite easily vary by many orders of magnitude. This is to be strongly contrasted with the situation where the diffusion coefficients themselves are required to differ by a large amount – the standard route to Turing patterns – since it is difficult to imagine realistic situations where this holds true.

The biological mechanism we propose here is analogous to the mechanism proposed as an explanation for the chlorite-iodide-malonic acid-starch reaction system, which was the first chemical system in which Turing patterns were observed experimentally.[9] Lengyel and Epstein[10,11] showed that the existence of Turing patterns in this system, despite the similar diffusion coefficients of the reactants, is a consequence of the binding and unbinding of iodine to starch molecules that have been immobilized by the gel which serves as an "inert" medium of the reaction. What we are proposing here is a biologically realistic and necessary mechanism that is able to provide just this type of effect in living cells.

Setting $A(\mathbf{x},t) = [A]$, $I(\mathbf{x},t) = [I]$ $M_A(\mathbf{x},t) = [M_o]$ and $M_I(\mathbf{x},t) = [M_I]$ to be the concentration at a given time t and position $\mathbf{x}$, we can write down the following set of four

reaction-diffusion equations

$$\partial_t A = c_A - \lambda_A A + \frac{V_1 A}{K_1 + A} - \frac{V_3 A I}{K_3 + A} - \alpha_A A + \beta_A M_A - \epsilon \nabla^2 A, \tag{5}$$

$$\partial_t I = c_I - \lambda_I I + \frac{V_2 A}{K_2} - \alpha_I I + \beta_I M_I - \epsilon \nabla^2 I, \tag{6}$$

$$\partial_t M_A = \alpha_A A - \beta_A M_I - D \nabla^2 M_A, \tag{7}$$

$$\partial_t M_I = \alpha_I I - \beta_I M_I - D \nabla^2 M_I. \tag{8}$$

Here ϵ is a very small (or negligible) rate of diffusion arising from "leakage" though the cell membrane which occurs very rarely. We introduce this small quantity for a mathematical reasons in order to give the first two equations a spatial scale and to remove the singular nature of the limit where $\epsilon = 0$. However we emphasize that the model still forms patterns even when $\epsilon = 0$ (see Fig. 2).

For the purposes of keeping our illustration as simple as possible we will specifically consider only the case where $c_A = c_I = 1$, $\alpha_A = \beta_A = 1$ and $\alpha_I = \beta_I = \rho$. We further set limiting velocities of the catalyzed reactions to $V_1 = 500$, $V_2 = 1$, and $V_3 = 60$, and the parameters $\lambda_A = 1/100$, $\lambda_I = 7$, $K_1 = 100$, $K_2 = 1$, and $K_3 = 1/10$. For this model the stationary homogenous state is $A(\mathbf{x}) = M_A(\mathbf{x}) \simeq 2.46$ and $I(\mathbf{x}) = M_I(\mathbf{x}) \simeq 2.25$. A standard linear stability[2] analysis of Eqs. (1-4) about this state tells us that an initial perturbation of the uniform state with a given wave vector $\mathbf{k}$ will have an amplitude that grows (or shrinks)

in proportion to the factor $e^{\lambda_k t}$, where λ_k are eigenvalues of the stability matrix

$$\tilde{\mathbf{S}} = \begin{bmatrix} 3.55 - \epsilon k^2 - 1 & -5.77 & 1 & 0 \\ 6 & -7 - \rho - \epsilon k^2 & 0 & \rho \\ 1 & 0 & -1 - k^2 & 0 \\ 0 & \rho & 0 & -\rho - k^2 \end{bmatrix}, \tag{9}$$

and can be real or come in complex conjugate pairs. Each value of k corresponds to a spatial mode with wavelength $L = 2\pi\sqrt{D}/k$. The real parts of the eigenvalues corresponding to this mode, $\Re(\lambda_k)$, determine the stability of perturbations away from the homogeneous state with the corresponding wavelength: $\Re(\lambda_k) < 0$ indicates the mode is stable, and $\Re(\lambda_k) > 0$ indicates an unstable mode which will grow when a small random fluctuation displaces it from equilibrium. Thus the existence of a wave number k such that $\lambda_k > 0$ means patterns will form. Turing patterns occur when the largest eigenvalue is real ($\Im(\lambda_k) = 0$) which is the case for the parameters we have chosen here. The largest eigenvalue has a negative real part ($\Re(\lambda_k) < 0$) when $D \to 0$ showing that the system is globally stable in the absence of diffusion.

The type of patterns that form will depend to a large degree on the spectrum of unstable k modes; it especially depends on the mode with the greatest λ_k, but also on the range of other unstable modes. As was mentioned above, we included a small diffusion effect *through* the membrane with diffusion coefficient ϵ for mathematical reasons in order to remove the singular nature of the equations when the diffusion vanishes. In Fig. 2(B) we show the effect of varying ϵ on the frequency spectrum. As $\epsilon \to 0$ the spectrum of unstable modes is

broadened towards the higher frequency modes until at $\epsilon = 0$, the maximum k value in the spectrum goes to infinity. Physically this means that shorter and shorter wavelengths will come to dominate, and at some point the wavelength of the patterning will be limited by the finite dimension of the cells.

Fig. 3 shows some of the ordered patterns that emerge spontaneously in the system we studied for varying values of ρ ranging from (A) "honeycomb" ($\rho = 6$) to (B) stripes ($\rho = 11.5$) to (C) spots ($\rho = 100$). Our system is capable of supporting more or less the same patterns as an ordinary Turing mechanism that uses widely differing diffusion coefficients. The principal difference is that our mechanism provides a physiologically and chemically feasible route by which a wide range of patterns could arise.

Previous work has shown that pattern formation can occur in some systems with equal diffusion coefficients, but only if there is some kind of initial asymmetry such as a finite size perturbation[12] or an external advective flow.[13,14] These mechanisms might provide useful models for subsequent morphogenetic events in the embryo where some spatial genetic patterning or chemical gradients have already been set up, but still does not provide an adequate explanation of initial pre-patterning events which may start from a completely homogeneous initial state. The existence of an organizing center begs the question of how the center itself formed.

Our model provides a possible, physiologically realistic route to symmetry *breaking* instabilities in cellular systems, and we hope that it will provide a useful context in which to explore the possible relevance of Turing mechanisms to cellular morphogenesis. For in-

stance, our model makes a clear distinction between reacting and diffusing entities and thus provided somewhat different expectations for making experimental observations. The messengers could be almost any type of molecule, and are not required to have any complex reactive chemical properties. Rather, it is the properties of the transmitter and receiver proteins in the signal transduction pathway that will control the pattern formation. As a consequence it may be unproductive to search for specific "morphogens" since the biochemical substances that differentiate spatial patterns in a collection of cells may be unrelated to the substances that actually mediate the cell-to-cell communication.

M.M. is supported by a Whitaker Foundation award. E.R. is supported by a National Science Foundation Graduate Fellowship.

References

1. Turing, A. M. The Chemical Basis of Morphogenesis. *Phil. Trans. Royal Soc.* **B 237**, 37-72 (1952).

2. Meinhardt, H. *Models of Biological Pattern Formation* (London: Academic Press, 1982).

3. Koch, A. J. & Meinhardt, H. Biological Pattern Formation. *Rev. Modern Phys.* **66**, 1481-1507 (1994).

4. Kondo, S. & Asai., R. A reaction-diffusion wave on the skin of the marine angelfish Pomacanthus. *Nature* **376**, 765-768 (1995).

5. Glansdorff, P. & I. Prigogine. *Thermodynamics Theory of Structure, Stability and Fluctuations* (London: John Wiley & Sons, 1971).

6. Gierer, A. & Meinhardt, H. A theory of biological pattern formation. *Kybernetik* **12**, 30-39 (1972).

7. Segel, L. A. & Jackson, J. L. Dissipative structure: an explanation and an ecological example, *J. Theor. Biol.* **37**, 545-459.

8. Fersht, A. *Enzyme Structure and Function* (New York: W. H. Freeman, 1984).

9. Castes, V., Dulos, E., Boissonade, J. & P. De Kepper. Experimental evidence of a sustained standing Turing-type nonequilibrium chemical pattern. *Phys. Rev. Lett.* **64**, 2953-2956 (1990).

10. Lengyel, I. & Epstein, I. R. Modeling of Turing structures in the chlorite-iodide-malonic acid-starch reaction system. *Science* **251**, 650-652 (1991).

11. Lengyel, I. & Epstein, I. R. A chemical approach to designing Turing patterns in reaction-diffusion systems. *Proc. Natl. Acad. Sci.* **89**, 3977-3979 (1992).

12. Vastano, J. A., Pearson, J. E., Horsthemke, W. & Swinney, H. L. Chemical Pattern Formation with Equal Diffusion Coefficients. *Phys. Lett. A* **124**, 320-324 (1987).

13. Rovinsky, A. B. & Menzinger, M. Chemical Instability Induced by a Differential Flow. *Phys. Rev. Lett.* **69**, 1193-1196 (1992).

14. Rovinsky, A. B. & Menzinger, M. Self-Organization Induced by the Differential Flow of Activator and Inhibitor. *Phys. Rev. Lett.* **70**, 778-781 (1993).

Figure Legends

Figure 1: General kinetic schematic for model. The three basic kinetic elements of our model are shown. The simplified reactions in the cytosol involve an activator substance A and inactivator I which are created at constant rates by the cell and likewise broken down at the rates λ_A and λ_I. In this case trans-membrane signal transduction takes the form of transformation of A and I in the cytosol (mediated by the membrane proteins T_A and T_I) into corresponding messenger molecules M_A and M_I in the extracellular matrix. Likewise R_A and R_I mediate the reverse transformation. Both of the messenger substance diffuse at rate D through the extracellular matrix.

Figure 2: Linear stability spectrum of the model. The dotted lines indicate regions where the eigenvalue with the largest real part is complex. Parametet given in the text. (A) shows the spectrum of stability eigenvalues for several values of the critical parameter ρ. For $\rho < 3.5$ all the eigenvalues have negative real parts, and the homogeneous distribution of reactants is stable. Turing patterns set in when $\rho > 3.5$, and a range of frequency modes become unstable, giving rise to spontaneous ordering. (B) shows the effect on the spectrum when $\rho = 5$ as ϵ is varied. As $\epsilon \to 0$, the most unstable mode shifts to higher and higher frequencies, but ordering will still take place.

Figure 3: Turing Patterns (A) Concentrations of activator and inhibitor within cells at $t = 125$ for $\rho = 6$. Concentration were set to zero at $t = 0$ and allowed to build up naturally,

the situation that would arise if the genes for the production of A and I were suddenly switched on at $t = 0$. The activator is shown as shades of green (black indicating 0 and green the maximum value, here 32.0), and the inhibitor as shades of red (black = 0 to red = 21.3) as shown in the legend (D). The two are superimposed so that yellow indicates the presence of both activator and inhibitor. $D = 600$, $\epsilon = D/100$; the grid size is 100. (B) Concentrations of A and I at $t = 40$ for $\rho = 11.5$ and other parameters as above. $A_{max} = 53.8$ and $I_{max} = 28.4$. (C) Concentrations of A and I at $t = 40$ for $\rho = 100$. $A_{max} = 117.6$ and $I_{max} = 35.3$.

Numerical Method: The reaction component of the equations was integrated using a forward-Euler method. The Laplacian (diffusion) term was implemented using the following conservative method: for each pair of locations $\{i, j\}$, $A_i(t+1) = A_i(t) + \Delta A; A_j(t+1) = A_j(t) - \Delta A$ where $\Delta A = M_{ij} D(A_i(t+1) f(i,t) - A_j(t+1) f(j,t))\Delta t$ and M_{ij} is the connectivity matrix. The noise function f is a uniformly distributed random variable, ranging from 0 to 10^{-5} and models the effect of very weak fluctuations of the type that are required to initiate the initial instability. We used a von Neumann neighborhood and toroidal boundary conditions.

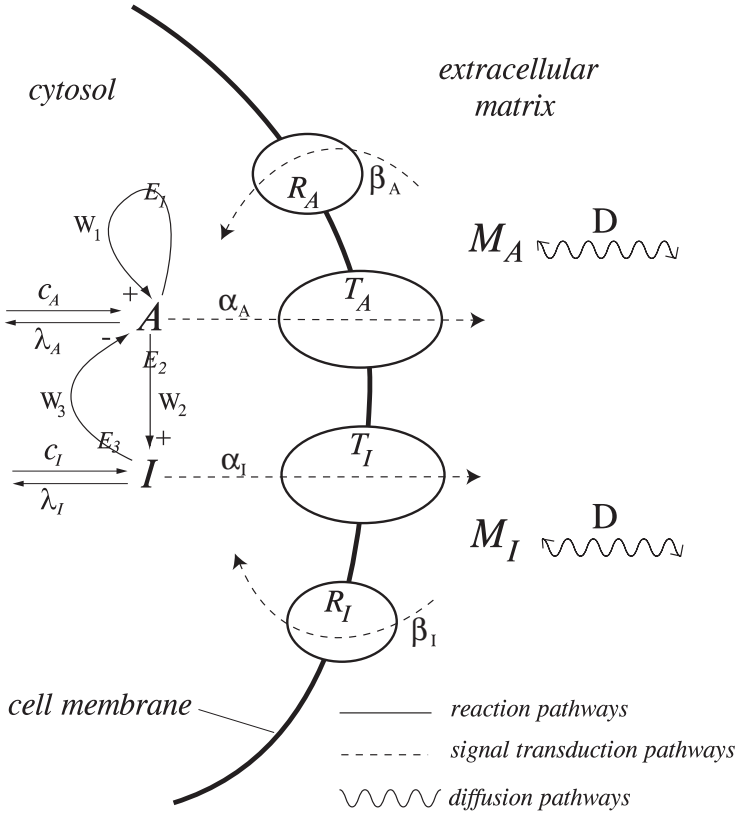

Figure 1

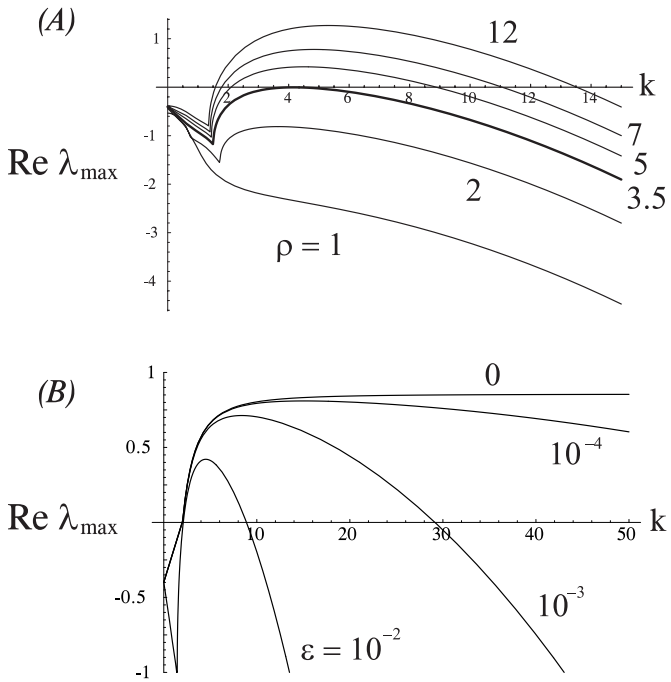

Figure 2

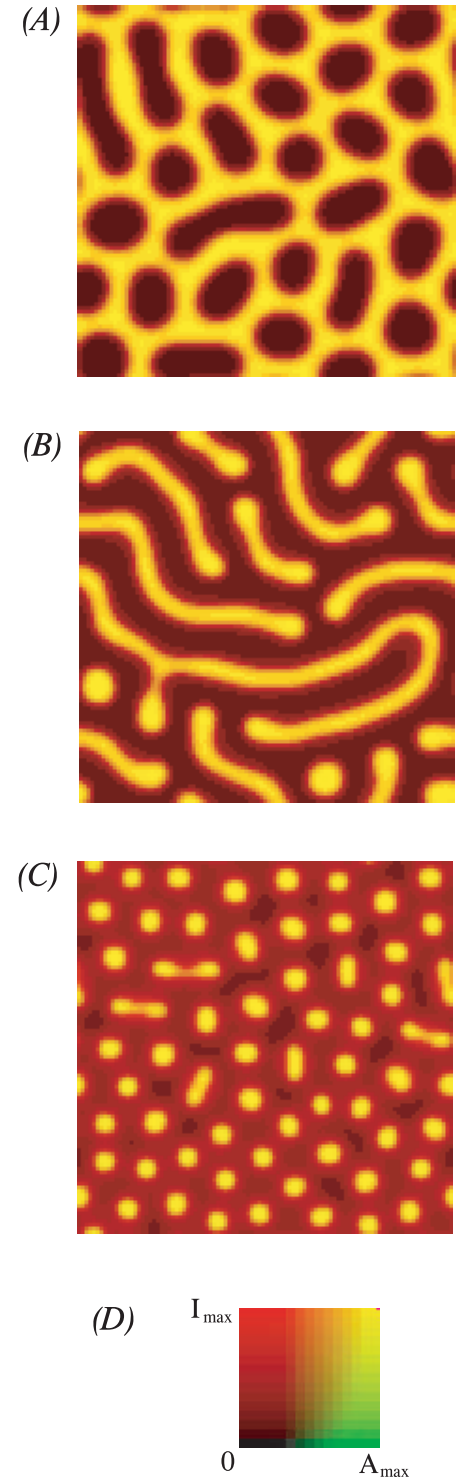

Figure 3

Figure 1: